Author Manuscript

Author Manuscript

Author Manuscript

Author Manuscript

HHS Public Access

Author manuscript

J Hum Genet. Author manuscript; available in PMC 2016 July 08.

Published in final edited form as:

J Hum Genet. 2016 May ; 61(5): 395–403. doi:10.1038/jhg.2015.160.

A patient with a novel homozygous missense mutation in *FTO* and concomitant nonsense mutation in *CETP*

Ahmet Okay Çağlayan[1,2,*,#], **Beyhan Tüysüz**[3,#], **Süleyman Coşkun**[1], **Jennifer Quon**[1], **Akdes Serin Harmanci**[1], **Jacob F. Baranoski**[1], **Burçin Baran**[1], **E. Zeynep Erson-Omay**[1], **Octavian Henegariu**[1], **Shrikant M. Mane**[4], **Kaya Bilgüvar**[5], **Katsuhito Yasuno**[1], and **Murat Günel**[1]

[1]Departments of Neurosurgery, Neurobiology and Genetics, Yale Program in Brain Tumor Research, Yale School of Medicine, New Haven, 06510, Connecticut, USA

[2]Department of Medical Genetics, School of Medicine, Istanbul Bilim University, Istanbul, 34394, Turkey

[3]Division of Genetics, Department of Pediatrics, Istanbul University Cerrahpasa Faculty of Medicine, Istanbul, 34098, Turkey

[4]Yale Center for Genomic Analysis, Yale University School of Medicine, New Haven, Connecticut 06520, USA

[5]Department of Genetics, Center for Human Genetics and Genomics and Program on Neurogenetics, Yale School of Medicine, New Haven, 06510, Connecticut, USA

Abstract

The fat mass and obesity associated gene (*FTO*) has previously been associated with a variety of diseases and conditions, notably obesity, acute coronary syndrome and metabolic syndrome. Reports describing mutations in *FTO* as well as FTO animal models have further demonstrated a role for FTO in the development of the brain and other organs. Here, we describe a patient born of consanguineous union who presented with microcephaly, developmental delay, behavioral abnormalities, dysmorphic facial features, hypotonia, and other various phenotypic abnormalities. Whole exome sequencing revealed a novel homozygous missense mutation in *FTO* and a nonsense mutation in the cholesteryl ester transfer protein (*CETP*). Exome CNV analysis revealed no disease causing large duplications or deletions within coding regions. Patient's, her parents' and non-related control' fibroblasts were analyzed for morphologic defects, abnormal proliferation, apoptosis and transcriptome profile. We have shown that FTO is located in nucleus of cells from each tested samples. Western blot analysis demonstrated no changes in patient FTO. Q-PCR analysis revealed slightly decreased levels of FTO expression in patient cells compared to controls. No morphological or proliferation differences between the patient and control fibroblasts were observed. There is still much to be learned about the molecular mechanisms by which mutations in *FTO* contribute to such severe phenotypes.

Users may view, print, copy, and download text and data-mine the content in such documents, for the purposes of academic research, subject always to the full Conditions of use: http://www.nature.com/authors/editorial_policies/license.html#terms

[*]Corresponding author: ahmetokay.caglayan@istanbulbilim.edu.tr (AOC); ahmet.caglayan@yale.edu (AOC).
[#]Co-first authors

Author Manuscript Author Manuscript Author Manuscript Author Manuscript

Introduction

The fat mass and obesity associated (FTO) gene was the first gene locus reported to be associated with body weight and metabolic disorders [1–5]. Since then, a cluster of common variants in the first, and largest, intron of *FTO* have been described across multiple populations of different ethnicities [6–9]. Recently, Boissel et al. described a consanguineous Palestinian-Arab family with a homozygous non-synonymous *FTO* mutation that led to an inherited life-threatening disease in nine family members – this was the first report of a homozygous *FTO* mutation in the literature. The identified mutation resulted in an arginine to glutamine change at position 316 (R316Q) thereby rendering FTO catalytically inert [10]. The affected family members suffered from postnatal growth retardation, head and face dysmorphisms, severe psychomotor delay, functional cognitive deficits, and, in some patients, brain malformations, cardiac defects, genital abnormalities, and cleft palates. In all affected individuals, death occurred within the first 30 months of life. In this report, we describe a patient with a novel homozygous missense mutation in *FTO*. We further discuss the phenotypic expression of this mutation.

Materials and Methods

Ethics Statement

The study protocol was approved by the Yale School of Medicine Human Investigation Committee (HIC) (protocol number 0908005592). Institutional review board approval for genetic and MRI studies and written consent from all study subjects, were obtained by the referring physicians at participating institutions.

DNA Extraction

Blood samples were collected from patients and their parents. DNA was extracted from the blood using the commercially available Gentra Puregene Blood Kit from Qiagen.

Whole Genome Genotyping

Samples were analyzed using 610K Quad Bead Chips according to the manufacturer's protocol (Illumina).

Whole Exome Capture and Sequencing

Exome capture for the index case was performed using the NimbleGen 2.1M human exome array (Roche Nimblegen, Inc.) according to the manufacturer's protocol along with modifications previously described in the literature [11, 81]. Exome library sequencing was performed using the HiSeq2000 with barcoding technology, paired end analysis, and six samples per lane. Image analysis and subsequent base calling was performed using the Illumina pipeline (version 1.8).

Exome Data Analysis

Analysis of the sequencing data was performed according to the previously described bioinformatics pipeline devised by our research team [82].

Author Manuscript Author Manuscript Author Manuscript Author Manuscript

Sanger Sequencing

Coding regions and exon-intron boundaries of *FTO* were evaluated by Sanger sequencing using standard protocols. Amplicons were cycle sequenced on ABI 9800 Fast Thermo cyclers, and post cycle sequencing clean-up was carried out with the CleanSEQ System (Beckman Coulter Genomics). The amplicons were analyzed on 3730×L DNA Analyzer (Applied Biosystems Inc.).

Copy Number Variation (CNV) Analysis

The depth of coverage log ratio between the patient and control samples was calculated using the GATK-Depth of Coverage tool. Segments with CNVs were identified from the log ratio of the depth of coverage using the ExomeCNV R package [83]. False positive CNV events were identified and corrected for by calculating minor allele frequencies (BAF) in each CNV segment.

Co-Expression Analysis

Co-expression patterns were analyzed using the Database for Annotation, Visualization and Integrated Discovery (DAVID) v6.7 [84]. Interrogation and procurement of results were performed using previously established protocols [12, 13].

Skin Biopsy and Fibroblast Culture

Four millimeter skin punch biopsies were obtained from the umbilical area of the patient (NG1305-1), her parents (NG1305-2 and NG1305-3) as well as from control individuals using a standardized procedure [85, 86]. Samples were maintained in 50 ml conical tubes filled with Dulbecco's Modified Eagle Medium (DMEM; Gibco, cat. no. 11965-084) supplemented with 10% heat-inactivated fetal bovine serum (FBS; Gibco, cat. no. 10438-026), 1% (1x) L-glutamine (Gibco, cat. no. 25030-081), and 2% (1x) Penicillin-Streptomycin (Gibco, cat. No. 15140-122), and subsequently transported to the laboratory for culture. Once they arrived in the laboratory, samples were washed at least three times in PBS (*Sigma Chemical Co., Saint Louis, USA*). Samples were cut into small fragments and placed in 100 mm^2 Petri dishes, which were maintained for 30 minutes semi-opened in laminar flow to allow specimens to adhere to the dish surface. Afterwards, 10 ml of culture medium containing DMEM supplemented with 10% heat-inactivated fetal bovine serum, 1% (1x) L-glutamine, 1% (1x) Penicillin-Streptomycin at 37°C, was added to the dish. Cultures were maintained in a humidified incubator at 37°C, under 5% CO2 in air. The culture medium replaced initially after two days and, subsequently changed three times a week. Fibroblasts began to emerge from the biopsy fragments within in 7–9 days. Subculture (passage) of fibroblasts was performed at 70% cellular confluence.

Once there were sufficient cells, enzymatic detachment was performed using 0.25% Trypsin-EDTA (1X) (Gibco, cat. no. 25200-056) and cells were plated in 25 cm^2 culture flasks for additional proliferation. Primary fibroblasts were grown at 37°C in 5% CO2 and medium was changed every two days. Cells were passaged using trypsin at approximately 70% confluence and either harvested for cryopreservation or reseeded for further proliferation. Early passages of fibroblasts were used for cell-based functional assays.

Author Manuscript Author Manuscript Author Manuscript Author Manuscript

Population Doubling Assay

Cells were trypsinized upon confluency and 2000 cells per well were seeded in 135 microliters of medium. There were nine wells per individual (NG1305-1, NG1305-2, NG1305-3, CTRL-1, CTRL-2 and CTRL-3) included on a 96 well-plate. A separate plate of cells was also included using serial dilutions of cells for calibration curve. After 2^{nd}, 5^{th}, 7^{th}, 9^{th} and 11^{th} days of incubation, we performed a CellTiter-Glo® Luminescent Cell Viability Assay (Promega). Luminescence was read using the GloMax®-Multi Detection System (Promega) and data was analyzed with Graphpad Prism software.

Fibroblast Morphology and Apoptosis Assay

Fibroblasts were seeded in 24-well plates and images were obtained on the 2^{nd}, 5^{th}, 7^{th}, 9^{th} and 11^{th} days using an inverted microscobe at 20× magnification. Apoptosis was evaluated with an Annexin V-FITC and 7-amino-actinomysin (7-AAD) dye kit (Ebioscience) according to manufacturer's protocol. Briefly, cells were harvested and washed in 1X PBS, and then resuspended in 1X Binding Buffer at $1–5\times10^6$ cells/mL. 5 μL of fluorochrome-conjugated Annexin V was added to 100 μL of the cell suspension, which was then incubated 10–15 minutes at room temperature and protected from light. Cells were subsequently washed with 2 mL of 1X Binding Buffer and resuspended in 200 μL of 1X Binding Buffer. 5 μL of 7-AAD viability staining solution was added to the solution, which was stored at 2–8°C in the dark, and analyzed within 4 hours using flow cytometry.

Immunohistochemistry and Immunostaining

For immunohistochemistry of fibroblasts from extracted skin biopsies of index case, her parents and control sample were fixed in 3.6% formaldyhyde and washed three times with PBS. Then cells were exposed to 0.3% Triton X-100 (Sigma Chemical) in phosphate buffered saline for 1 minutes and then washed two times with PBS. Cells were blocked in blocking solution containing 1X phosphate buffered saline (PBS), 5% normal bovine serum, 5% normal goat serum, 5% normal donkey serum and 0.1% Tween for half an hour at room temperature. After blocking, specimen were extensively washed in PBS and incubated with primary antibodies diluted in blocking solution on a horizontal shaker overnight at 4°C, and washed in PBS at room temperature for three times. Cells were then incubated with secondary antibodies in blocking solution for 1 hours and washed in PBS for three times at room temperature, then washed and imaged with Zeiss microscopy system. Primary antibody used for immunohistochemistry are: a custom rabbit anti–recombinant mFTO antibody (1:100 dilution). Alexa Fluor®488 Donkey Anti-Rabbit IgG (H+L) Antibody (A-21206, Life technologies) was used as secondary antibody.

Western Blot Analysis

Protein expression was analyzed by Western blot analysis as described previously [87]. Proteins were extracted from fibroblasts of patient, her father and mother and control subject, then protein blots were performed on 40 μg of total proteins. The primary antibodies used were as follows: a custom rabbit anti–recombinant mFTO antibody (1:100 dilution), anti-glyceraldehyde 3-phosphate dehydrogenase (1:100 dilution, Rabbit, catalog no.: sc-25778, Santa Cruz Biotechnology, Santa Cruz, CA). The horseradish peroxidase (HRP)-

Author Manuscript Author Manuscript Author Manuscript Author Manuscript

conjugated secondary antibody used was as AffiniPure goat-anti-rabbit IgG FC-fragment was used (Jackson, West Grove, PA #111-035-046).

RNA Extraction, cDNA Synthesis and Quantitative PCR analysis

FTO mRNA expression in affected individual, both parents and control sample (individual of the same ethnicity and without a *FTO* sequence variant is used as control) was assessed by real-time-PCR (RT-PCR). Total RNA was isolated using miRNeasy Mini Kit (Qiagen; catalog no.: 24104) from fibroblasts according to the manufacturer's instructions and transcribed into complementary DNA (cDNA) as described previously (Applied Biosystems; catalog no.:4374966). RNA quantity was assessed using a NanoDrop spectrophotometer for cDNA synthesis. Quantitative PCR (qPCR) analysis was performed using FastStart Universal SYBR Green Master Mix (Roche; catalog no.: 04913914001). Two different *FTO* and the reference gene *TBP* (TATA box-binding protein) primers were used and the PCR efficiency of >90% (slope= −3.2 and −3.6) and R^2 99% obtained. Relative changes in gene expression were analyzed with the ΔCT method [88].

Transcriptome Analysis

To further characterize the effects of the *FTO* mutation in the family, RNA was extracted from these fibroblast cultures and RNA expression analysis using Illumina HumanHT12.v4 chips was performed on patient, father and mother samples and analyzed using the DAVID platform. Briefly, data is normalized using normal-exponential convolution model-based background correction and quantile normalization using the *limma* R package. The normalized data for 3 samples were used to perform an unsupervised hierarchical clustering using the euclidean distance as the dissimilarity metric and the average agglomerative method for clustering.

Results

Clinical Report

We report the case of a five year-old female (NG1305-1) presented with a dysmorphic face and developmental delay. She was the first child born of a consanguineous union (parents were second cousins) (Fig. 1). She was born at 40 weeks gestation with 2460 g (3rd percentile) and 50 cm long (50th percentile). Her head circumference at birth was not recorded. She was immediately admitted to the neonatal intensive care unit after birth due to respiratory distress and concern given her dysmorphic facial features. During her hospitalization she began to have seizures that were managed with antiepileptic medications. She was subsequently discharged, but was later admitted at nine and a half months-old. At this time, her weight was 7650 g (10th percentile), height was 66 cm (3rd percentile), and head circumference was 41 cm (<2nd percentile). On examination, she was hypertonic and lacked the ability to control her head movements. She was microcephalic, had sparse hair and eyebrows, a prominent metopic ridge, an asymmetric skull, esotropia of her right eye, hypotelorism, a long philtrum, microretrognathia, a high palate, a prominent alveolar ridge, anteverted nostrils, a thin vermillion and lips, and a short neck (Fig. 1B). She was noted to have hepatosplenomegaly and diastasis recti. Laboratory workup revealed high AST (70 U/L), ALT (57 U/L), and CK (1191 U/L) levels. Eye examination demonstrated bilateral

Author Manuscript Author Manuscript Author Manuscript Author Manuscript

nystagmus, iris nodules, posterior synechia, and astigmatism. Assessment of auditory brainstem responses demonstrated bilateral conductive and sensorineural hearing loss. At 19 months of age the patient's weight was 11 kg (<3rd percentile), height was 83.5 cm (<3rd percentile), and head circumference was 45cm (<3rd percentile). In addition to the previously noted physical exam findings, she was now also found to have difficulty swallowing. An echocardiogram was performed and demonstrated normal cardiac anatomy and function. Upper endoscopy revealed grade 1 esophageal varices. A head CT demonstrated prematurely closed metopic sutures (craniosynostosis). A brain MRI revealed a thin corpus callosum. Chromosomal analysis demonstrated a normal female karyotype. In addition to the physical exam abnormalities, the patient also demonstrated developmental delay with respect to reaching milestones – she did not develop head control until after 10 months of age, began sitting without support at 2 years-old, and walking at 4 years-old. Throughout this time, her AST, ALT and CK all remained abnormally elevated. A liver biopsy was performed but did not show any abnormalities; EMG was unremarkable. At 3 years-old, Denver testing confirmed severe developmental delay and the Wechsler Intelligence Scale for Children-Revised showed profound intellectual disability (IQ:23). At 4 years and 9 months, the patient's weight was 15 kg (10th percentile), height was 97cm (3rd-10th percentile), and head circumference was 46cm (<3rd percentile). She was microcephalic, could walk with support, and spoke a few words. The patient also continued to have bilateral nystagmus, brachydactyly and hepatosplenomegaly. Labs demonstrated a high CK (816 U/L, normal <170), normal total cholesterol (173 mg/dl, normal 114–200), low LDL cholesterol (30 mg/dl, normal 63–130), and high HDL cholesterol (136 mg/dl, normal 30–75) (S1 Table).

She was last time evaluated 5.5 years of age. She developed seizures at 5 years old and electroencephalogram demonstrated that high amplitude and irregular waves and spikes being more prominent on the right side of posterior temporal occipital region. After seizures she lost the ability to assisted walk assisted and spoken a few words. Six months after seizure when she was 5 years, 6 months old, she gained the ability of walk with support, however speech never came back. Her weight was 19kg (25–50th percentile), height was 100.5cm (3rd–10th percentile), and head circumference was 47cm (<3rd percentile). She had also suck/swallowing disorders, frequent drooling and protruding tongue. Physical exam was also remarkable for enlargement of both her liver and spleen (5 cm and 4 cm below costal margin, respectively). Repeated blood tests demonstrated a normal AST (29 U/L) and ALT (29 U/L) levels, high CK (587 U/L, normal <174), normal total cholesterol (153 mg/dl, normal 114–200), and high HDL cholesterol (127 mg/dl, normal 30–75). In addition, she demonstrated abnormal behavior phenotype such as repetitive hand movements, frequent laughter/smiling, apparent happy demeanor and short attention span. Evoked response audiometry (ERA) revealed that moderate hearing loss at right ear and mild hearing loss at left ear. Intriguingly, her father and mother had obesity, both weight were 100 kg. The father's height was 169 cm and the mother's height was 161 cm, father's head circumference was 58 cm, and mother's was 55 cm. Blood biochemistry analysis for parents of the patient revealed high total cholesterol levels (father 264 mg/dl, and mother 240 mg/dl), and high LDL cholesterol levels (father 169 mg/dl, mother 142.2 mg/dl) in both parents, however in father triglyceride levels also was found to be high (180 mg/dl). We also have found high

Author Manuscript Author Manuscript Author Manuscript Author Manuscript

HgA1c level (6.4) in father which indicates increased risk for type 2 diabetes. Both parents' blood HDL, glucose, cortisol and insulin levels were found within normal limits. Blood CPK level was normal for mother however was found to be high in father (438 mcg/L) which may be found high levels in different situations such as heart attack, myaocarditis, myopathy, hypo/hyperthyroidism etc. where problems occured normally found organs in where is mainly in the heart, brain, and skeletal muscle.

Whole Genome Genotyping and Whole Exome Sequencing

Whole genome genotyping was performed and the inbreeding coefficient for the patient (NG1305-1) was determined to be 0.01. Homozygous genomic segments (>2.5 cM each) were identified (S2 Table) and whole exome capture and sequencing of the patient's germ line DNA (S3 Table) was used to search for disease causing mutations within these regions [11].

Variant analysis identified only 2 homozygous novel mutations located within the aforementioned regions of homozygosity (S4 Table) (Fig. 1). The first was a homozygous missense mutation (ENST00000471389.1:c.812A>C) within the *FTO* (fat mass and obesity associated) coding sequence at position 53,878,127 on chromosome 16. This mutation resulted in a histidine to proline change at position 271 (ENSP00000418823.1:p.His271Pro) in the amino acid sequence of the FTO protein. This *FTO* mutation has not been previously reported in the dbSNP, NHLBI GO ESP Exome Variant Server, or 1000 Genomes databases, nor has it been observed within the cohort of 3,000 subjects with non-neurological diseases who have been whole-exome sequenced at the Yale School of Medicine. When we interrogated these databases for the mutational burden of *FTO*, we found no instances of homozygous deleterious mutations in *FTO*.

The other detected mutation (ENST00000566128.1:c.1207C>T) was in the *CETP* (cholesteryl ester transfer protein, plasma) gene at position 57,017,318 on chromosome 16, resulting in an early protein truncation and likely subsequent nonsense mediated decay (ENSP00000456276.1:p.Arg403X).

Sanger sequencing of the entire coding region of *FTO* and *CETP* in the patient's parents revealed that both were heterozygous for the identified mutations (Fig. 1). The parents were then reexamined for metabolic findings previously reported in association with *FTO* mutations but both were healthy and had no evidence of abnormal metabolic functioning. The patient's exome data was analyzed for large scale CNV events, and no disease causing large duplications or deletions within coding regions were identified (Fig. 1).

Co-Expression Data Analysis

Using the Human Brain Transcriptome database [12], we investigated the spatial and temporal changes in the *FTO* expression during human cortical development. *FTO* mRNA is expressed throughout the entire brain with marked expression in the fetal cortex and cerebellum. This expression remains robust in the adult brain (S1 Fig.) [12].

We next performed co-expression analysis on *FTO* [12, 13] (S5 and S6 Tables). We observed that *FTO* expression patterns positively correlate with the expression patterns of genes

Author Manuscript Author Manuscript Author Manuscript Author Manuscript

involved in the ubiquitin mediated proteolysis pathway such as *HUWE1, UBE3B,* and others. We also found that *FTO* expression patterns positively correlate with genes in which mutations cause either neurodevelopmental disorders such as *MECP2* (Rett syndrome, MIM:312750) and *GDI1* (Mental retardation, X-linked 41, MIM:300849), or hearing impairment such as *HARS* (Usher syndrome type 3B, MIM:614504).

Q-PCR, Western Blot, and Immunohistochemistry

We have shown that FTO is located in nucleus of cells from the patient, her parents, and non-related controls (Fig. 1). Western blot analysis demonstrated no changes in patient FTO, as expected given the observed mutation. Q-PCR analysis revealed slightly decreased levels of *FTO* expression in patient cells compared to controls (Fig. 1).

Transcriptome Analysis

Interestingly, we found that type 2 diabetes associated genes (insulin-like growth factor binding protein 2, 36kDa and neurocanthocytosis), retinol metabolism genes (*ALDH1A1*, *DHRS3* and *RDH10*), renin angiotensin system genes (*AGT* and *MME*), and genes related to metabolism of xenobiotics by cytochrome P450 (ALDH1A3, *GSTT1* and *MGST1*) demonstrated at least a twofold increase in relative expression in the patient's fibroblasts compared to her parents' and controls' fibroblasts. Conversely, cell cycle genes (*E2F2*, *BUB1*, *CDC20* and *CCNB1*), and obesity susceptibility genes (including *ADRB2, ENPP1*) demonstrated a relative decrease level of expression of at least 2-fold in the patients cells relative to her parents' and controls' samples.

Fibroblast Morphology, Population doubling, and Apoptosis Assays

Fibroblast morphology was compared among the patient (NG1305-1), parent (NG1305-2 and NG1305-3), and control cultures at 11 days incubation. No morphological differences between the patient and control fibroblasts were observed (Fig. 2). The rates of apoptosis were assessed at five and nine days incubation; again, no differences were appreciated between patient and control fibroblasts (Fig. 3). In addition, fibroblasts were counted on the 2^{nd}, 5^{th}, 7^{th}, 9^{th} and 11^{th} days and a growth curve was drawn (number of cells versus time) in order to calculate the population doublings (PD) from the exponential phase of the curve.

The PD, which occurred between the 5^{th} and 11^{th} days, was obtained using the equation: PD = (logN1/log2) - (logN0/log2), where N1 was the final and N0 was the initial cell count. There were no differences in proliferation between patient and control fibroblasts (Fig. 2, S7 Table).

Discussion

The FTO gene encompasses a large genomic region whose nine exons span more than 400 kb on chromosome 16q12.2 and encodes 505 amino acids FTO protein composed of two domains: an N-terminal domain carrying a catalytic core and a C-terminal domain of unknown function [14]. In our patient, as well as in the previously reported case, the homozygous *FTO* mutation affected the catalytic domain of the protein. Using both bioinformatic and *in vitro* biochemical data, *FTO* was predicted and confirmed to be an

Author Manuscript Author Manuscript Author Manuscript Author Manuscript

AlkB family DNA/RNA demethylase [15–17]. It has been known that the FTO protein localizes to the nucleus [15, 18, 19]. However, recently Gulati et al. demonstrated that a fraction of FTO located in the cytoplasm and N-terminus of FTO is necessary for its ability to shuttle between the nucleus and cytoplasm [20, 21]. Our IHC data demonstrating that FTO was localized to the nucleus of fibroblasts are consistent with this observation.

FTO expression begins early embryogenesis when it is ubiquitously expressed throughout the body, but it most highly expressed in the brain, which is consistent with the observation that multiple organ systems are affected by *FTO* deficiency [10, 15, 22]. Similar to the *FTO* phenotype previously reported by Boissel et al., our patient also demonstrated intrauterine growth retardation, failure to thrive, hypertonicity, seizures, severe developmental delay, postnatal microbrachycephaly, dysmorphic craniofacium, sensory-neural hearing loss, and optic disc abnormality, a short neck, cutis marmorata, a PDA, drumstick fingers, brachydactyly. Interestingly, not all of the affected family members demonstrated all of these traits and our case's clinical findings are less aggressive than Boissel et al cases' especially the ones who dies due to recurrent infections. Our patient additionally had abnormal behavior phenotype including repetitive hand movements, frequent laughter/smiling, apparent happy demeanor and short attention span as well as other clinical findings such as hip dislocation, strabismus, a trigonocephaly, thin upper and lower lips, a long philtrum, and osteopenia.

Because of its well-known association with obesity, *FTO* is well-studied [23–49]. Previous studies, have shown that even though some are predicted to have deleterious effects on FTO function, nonsynonymous mutations were equally common in both the obese and lean cohorts [50–52]. Other studies in lean and obese cohorts of children brought similar findings. In both African American and Chinese Han populations, variants were identified in *FTO*, but the overall frequencies were similar in case and control, with none conferring risk of obesity [53, 54].

Further, Boissel et al. reported none of the parents were appeared to be obese and detailed phenotypic data on the extended family has not been reported, in our case both of the parents of the affected children were obese, interestingly based on international diabetes foundation's (IDF) metabolic syndrome criteria, patients' father diagnosed as a metabolic syndrome due to his increased wrist circumference and blood pressure and high trigliceride level. Since patient's mother is also carrier for same *FTO* gene variant, father's metabolic syndrome may be caused by either environmental factors and/or sex selection for the metabolic result of *FTO* variant.

Variants in *FTO* and its association with various human phenotypes continue to emerge [6, 7, 9, 11, 55–63]. Intriguingly, in humans with loss-of-function mutations in *FTO* share phenotypic features of cases with partial trisomies of chromosome 16q including the *FTO* gene such as learning difficulties and behavioral problems [64, 65].

Boissel et al. demonstrated changed morphology, impaired proliferation and accelerated senescence in cultured skin fibroblasts from affected subjects. Although we did not test senescence, we were not able to detect any abnormalities in either morphology or

Author Manuscript Author Manuscript Author Manuscript Author Manuscript

proliferation in the patient fibroblast cultures compared to either parent or control fibroblasts. Given that we did not detect any defects in proliferation, we also tested for variability in the rates of apoptosis, and again did not see any statistically significant differences between the patient and parental.

Our patient was found to have a novel homozygous nonsense mutation in *CETP*, resulting in a truncated 403 amino acid protein (compared to the normal 476 amino acid protein), and likely causing a complete CETP deficiency. Human CETP is a 74kDa plasma glycoprotein that facilitates the transfer of cholesteryl esters between lipoproteins [68, 69]. Genetic deficiency of cholesteryl ester transfer protein (CETP) (OMIM 607322) is well known cause of primary, also known as familial, hyperalphalipoproteinemia (HALP), and results in elevated plasma HDL (2–5× increase in the homozygous and 25–80% greater in the heterozygous genotype) and decreased LDL [70–72] and it is mostly detected in the Japanese population more than Caucasians [72–74]. In Caucasians only a few cases of HALP due to *CETP* mutations have been reported [75–79]. Despite the high HDL-C levels in patients with CETP deficiency, an increased risk of atherosclerotic coronary artery disease (CAD) has been reported [80]. Our patient's mutation in *CETP* was novel and laboratory findings fit with the genetic diagnosis.

Boissel et al. were the first to report its homozygous loss of function mutation as an example of a human disorder related to a defect in an AlkB-related protein. We describe the second novel homozygous missense mutation in *FTO* to be reported in the literature, in addition to a nonsense mutation in *CETP*. We further discuss some of the phenotypic consequences of such an *FTO* mutation. However based on studies conducted in human and other organisms fully functional FTO is critical for normal physiology and there is still much to be learned about the molecular mechanisms by which a mutation *FTO* leads to such a severe phenotype, as observed in our and previously reported patients.

Supplementary Material

Refer to Web version on PubMed Central for supplementary material.

Acknowledgments

We thank the family for participating in this study. We would like thank to Professor Roger Cox and Dr Chris Church for providing FTO antibody, Nihal Hatipoglu, Ketu Mishra and A. Gulhan Ercan-Sencicek for technical assistance.

References

1. Fawcett KA, Barroso I. The genetics of obesity: FTO leads the way. Trends Genet. 2010; 26:266–274. [PubMed: 20381893]
2. Larder R, Cheung MK, Tung YC, Yeo GS, Coll AP. Where to go with FTO? Trends in endocrinology and metabolism: TEM. 2011; 22:53–59. [PubMed: 21131211]
3. Frayling TM, Timpson NJ, Weedon MN, Zeggini E, Freathy RM, Lindgren CM, et al. A common variant in the FTO gene is associated with body mass index and predisposes to childhood and adult obesity. Science. 2007; 316:889–894. [PubMed: 17434869]

Author Manuscript Author Manuscript Author Manuscript Author Manuscript

4. Speliotes EK, Willer CJ, Berndt SI, Monda KL, Thorleifsson G, Jackson AU, et al. Association analyses of 249,796 individuals reveal 18 new loci associated with body mass index. Nat Genet. 2010; 42:937–U953. [PubMed: 20935630]
5. Dina C, Meyre D, Gallina S, Durand E, Korner A, Jacobson P, et al. Variation in FTO contributes to childhood obesity and severe adult obesity. Nat Genet. 2007; 39:724–726. [PubMed: 17496892]
6. Gustavsson J, Mehlig K, Leander K, Lissner L, Bjorck L, Rosengren A, et al. FTO Genotype, Physical Activity and Coronary Heart Disease Risk in Swedish Men and Women. Circulation. Cardiovascular genetics. 2014
7. Liguori R, Labruna G, Alfieri A, Martone D, Farinaro E, Contaldo F, et al. The FTO gene polymorphism (rs9939609) is associated with metabolic syndrome in morbidly obese subjects from southern Italy. Molecular and cellular probes. 2014
8. Zermeño-Rivera JJ. Association of the FTO gene SNP rs17817449 with body fat distribution in Mexican women. Genetics and molecular research. 2014; 13
9. He D, Fu M, Miao S, Hotta K, Chandak GR, Xi B. FTO gene variant and risk of hypertension: A meta-analysis of 57,464 hypertensive cases and 41,256 controls. Metabolism: clinical and experimental. 2014
10. Boissel S, Reish O, Proulx K, Kawagoe-Takaki H, Sedgwick B, Yeo GSH, et al. Loss-of-Function Mutation in the Dioxygenase-Encoding FTO Gene Causes Severe Growth Retardation and Multiple Malformations. Am J Hum Genet. 2009; 85:106–111. [PubMed: 19559399]
11. Bilguvar K, Ozturk AK, Louvi A, Kwan KY, Choi M, Tatli B, et al. Whole-exome sequencing identifies recessive WDR62 mutations in severe brain malformations. Nature. 2010; 467:207–U293. [PubMed: 20729831]
12. Kang HJ, Kawasawa YI, Cheng F, Zhu Y, Xu X, Li M, et al. Spatio-temporal transcriptome of the human brain. Nature. 2011; 478:483–489. [PubMed: 22031440]
13. Huang DW, Sherman BT, Lempicki RA. Systematic and integrative analysis of large gene lists using DAVID bioinformatics resources. Nat Protoc. 2009; 4:44–57. [PubMed: 19131956]
14. Han Z, Niu T, Chang J, Lei X, Zhao M, Wang Q, et al. Crystal structure of the FTO protein reveals basis for its substrate specificity. Nature. 2010; 464:1205–1209. [PubMed: 20376003]
15. Gerken T, Girard CA, Tung YCL, Webby CJ, Saudek V, Hewitson KS, et al. The obesity-associated FTO gene encodes a 2-oxoglutarate-dependent nucleic acid demethylase. Science. 2007; 318:1469–1472. [PubMed: 17991826]
16. Jia G, Yang CG, Yang S, Jian X, Yi C, Zhou Z, et al. Oxidative demethylation of 3-methylthymine and 3-methyluracil in single-stranded DNA and RNA by mouse and human FTO. FEBS letters. 2008; 582:3313–3319. [PubMed: 18775698]
17. Wu Q, Saunders RA, Szkudlarek-Mikho M, de la Serna I, Chin KV. The obesity-associated Fto gene is a transcriptional coactivator. Biochemical and biophysical research communications. 2010; 401:390–395. [PubMed: 20858458]
18. Berulava T, Ziehe M, Klein-Hitpass L, Mladenov E, Thomale J, Ruther U, et al. FTO levels affect RNA modification and the transcriptome. European journal of human genetics : EJHG. 2013; 21:317–323. [PubMed: 22872099]
19. Jia GF, Fu Y, Zhao X, Dai Q, Zheng GQ, Yang Y, et al. N6-Methyladenosine in nuclear RNA is a major substrate of the obesity-associated FTO. Nat Chem Biol. 2011; 7:885–887. [PubMed: 22002720]
20. Gulati P, Cheung MK, Antrobus R, Church CD, Harding HP, Tung YC, et al. Role for the obesity-related FTO gene in the cellular sensing of amino acids. Proc Natl Acad Sci U S A. 2013; 110:2557–2562. [PubMed: 23359686]
21. Gulati P, Avezov E, Ma M, Antrobus R, Lehner PJ, O'Rahilly S, et al. Fat mass and obesity related (FTO) shuttles between the nucleus and cytoplasm. Bioscience reports. 2014
22. Stratigopoulos G, Padilla SL, Leduc CA, Watson E, Hattersley AT, McCarthy MI, et al. Regulation of Fto/Ftm gene expression in mice and humans. Am J Physiol-Reg I. 2008; 294:R1185–R1196.
23. Tung YC, Yeo GS, O'Rahilly S, Coll AP. Obesity and FTO: Changing Focus at a Complex Locus. Cell metabolism. 2014; 20:710–718. [PubMed: 25448700]

Author Manuscript Author Manuscript Author Manuscript Author Manuscript

24. Bradfield JP, Taal HR, Timpson NJ, Scherag A, Lecoeur C, Warrington NM, et al. A genome-wide association meta-analysis identifies new childhood obesity loci. Nat Genet. 2012; 44:526. [PubMed: 22484627]
25. Graff M, Ngwa JS, Workalemahu T, Homuth G, Schipf S, Teumer A, et al. Genome-wide analysis of BMI in adolescents and young adults reveals additional insight into the effects of genetic loci over the life course. Hum Mol Genet. 2013; 22:3597–3607. [PubMed: 23669352]
26. Lindgren CM, Heid IM, Randall JC, Lamina C, Steinthorsdottir V, Qi L, et al. Genome-wide association scan meta-analysis identifies three Loci influencing adiposity and fat distribution. PLoS genetics. 2009; 5:e1000508. [PubMed: 19557161]
27. Loos RJF, Yeo GSH. The bigger picture of FTO-the first GWAS-identified obesity gene. Nat Rev Endocrinol. 2014; 10:51–61. [PubMed: 24247219]
28. Meyre D, Delplanque J, Chevre JC, Lecoeur C, Lobbens S, Gallina S, et al. Genome-wide association study for early-onset and morbid adult obesity identifies three new risk loci in European populations. Nat Genet. 2009; 41:157–159. [PubMed: 19151714]
29. Scherag A, Dina C, Hinney A, Vatin V, Scherag S, Vogel CI, et al. Two new Loci for body-weight regulation identified in a joint analysis of genome-wide association studies for early-onset extreme obesity in French and german study groups. PLoS genetics. 2010; 6:e1000916. [PubMed: 20421936]
30. Speliotes EK, Willer CJ, Berndt SI, Monda KL, Thorleifsson G, Jackson AU, et al. Association analyses of 249,796 individuals reveal 18 new loci associated with body mass index. Nat Genet. 2010; 42:937–948. [PubMed: 20935630]
31. Thorleifsson G, Walters GB, Gudbjartsson DF, Steinthorsdottir V, Sulem P, Helgadottir A, et al. Genome-wide association yields new sequence variants at seven loci that associate with measures of obesity. Nat Genet. 2009; 41:18–24. [PubMed: 19079260]
32. Wheeler E, Huang N, Bochukova EG, Keogh JM, Lindsay S, Garg S, et al. Genome-wide SNP and CNV analysis identifies common and low-frequency variants associated with severe early-onset obesity. Nat Genet. 2013; 45:513–U576. [PubMed: 23563609]
33. Willer CJ, Speliotes EK, Loos RJF, Li SX, Lindgren CM, Heid IM, et al. Six new loci associated with body mass index highlight a neuronal influence on body weight regulation. Nat Genet. 2009; 41:25–34. [PubMed: 19079261]
34. Horikoshi M, Yaghootkar H, Mook-Kanamori DO, Sovio U, Taal HR, Hennig BJ, et al. New loci associated with birth weight identify genetic links between intrauterine growth and adult height and metabolism. Nat Genet. 2013; 45:76–U115. [PubMed: 23202124]
35. Jess T, Zimmermann E, Kring SII, Berentzen T, Holst C, Toubro S, et al. Impact on weight dynamics and general growth of the common FTO rs9939609: a longitudinal Danish cohort study. Int J Obesity. 2008; 32:1388–1394.
36. Kilpelaeinen TO, den Hoed M, Ong KK, Grontved A, Brage S, Jameson K, et al. Obesity-susceptibility loci have a limited influence on birth weight: a meta-analysis of up to 28,219 individuals. Am J Clin Nutr. 2011; 93:851–860. [PubMed: 21248185]
37. Hardy R, Wills AK, Wong A, Elks CE, Wareham NJ, Loos RJF, et al. Life course variations in the associations between FTO and MC4R gene variants and body size. Hum Mol Genet. 2010; 19:545–552. [PubMed: 19880856]
38. Sovio U, Mook-Kanamori DO, Warrington NM, Lawrence R, Briollais L, Palmer CNA, et al. Association between Common Variation at the FTO Locus and Changes in Body Mass Index from Infancy to Late Childhood: The Complex Nature of Genetic Association through Growth and Development. PLoS genetics. 2011; 7
39. Cecil JE, Tavendale R, Watt P, Hetherington MM, Palmer CN. An obesity-associated FTO gene variant and increased energy intake in children. The New England journal of medicine. 2008; 359:2558–2566. [PubMed: 19073975]
40. Speakman JR, Rance KA, Johnstone AM. Polymorphisms of the FTO gene are associated with variation in energy intake, but not energy expenditure. Obesity. 2008; 16:1961–1965. [PubMed: 18551109]

Author Manuscript Author Manuscript Author Manuscript Author Manuscript

41. Timpson NJ, Emmett PM, Frayling TM, Rogers I, Hattersley AT, McCarthy MI, et al. The fat mass- and obesity-associated locus and dietary intake in children. Am J Clin Nutr. 2008; 88:971–978. [PubMed: 18842783]
42. Park SL, Cheng I, Pendergrass SA, Kucharska-Newton AM, Lim U, Ambite JL, et al. Association of the FTO obesity risk variant rs8050136 with percentage of energy intake from fat in multiple racial/ethnic populations: the PAGE study. American journal of epidemiology. 2013; 178:780–790. [PubMed: 23820787]
43. Sonestedt E, Roos C, Gullberg B, Ericson U, Wirfalt E, Orho-Melander M. Fat and carbohydrate intake modify the association between genetic variation in the FTO genotype and obesity. Am J Clin Nutr. 2009; 90:1418–1425. [PubMed: 19726594]
44. Tanaka T, Ngwa JS, van Rooij FJA, Zillikens MC, Wojczynski MK, Frazier-Wood AC, et al. Genome-wide meta-analysis of observational studies shows common genetic variants associated with macronutrient intake. Am J Clin Nutr. 2013; 97:1395–1402. [PubMed: 23636237]
45. Wardle J, Carnell S, Haworth CMA, Farooqi IS, O'Rahilly S, Plomin R. Obesity associated genetic variation in FTO is associated with diminished satiety. J Clin Endocr Metab. 2008; 93:3640–3643. [PubMed: 18583465]
46. Wardle J, Llewellyn C, Sanderson S, Plomin R. The FTO gene and measured food intake in children. Int J Obesity. 2009; 33:42–45.
47. Tanofsky-Kraff M, Han JC, Anandalingam K, Shomaker LB, Columbo KM, Wolkoff LE, et al. The FTO gene rs9939609 obesity-risk allele and loss of control over eating. Am J Clin Nutr. 2009; 90:1483–1488. [PubMed: 19828706]
48. Kilpelainen TO, Qi L, Brage S, Sharp SJ, Sonestedt E, Demerath E, et al. Physical Activity Attenuates the Influence of FTO Variants on Obesity Risk: A Meta-Analysis of 218,166 Adults and 19,268 Children. Plos Med. 2011; 8
49. Yang J, Loos RJF, Powell JE, Medland SE, Speliotes EK, Chasman DI, et al. FTO genotype is associated with phenotypic variability of body mass index. Nature. 2012; 490:267. [PubMed: 22982992]
50. Meyre D, Proulx K, Kawagoe-Takaki H, Vatin V, Gutierrez-Aguilar R, Lyon D, et al. Prevalence of loss-of-function FTO mutations in lean and obese individuals. Diabetes. 2010; 59:311–318. [PubMed: 19833892]
51. Deliard S, Panossian S, Mentch FD, Kim CE, Hou CP, Frackelton EC, et al. The Missense Variation Landscape of FTO, MC4R, and TMEM18 in Obese Children of African Ancestry. Obesity. 2013; 21:159–163. [PubMed: 23505181]
52. Zheng ZJ, Hong L, Huang XD, Yang PR, Li J, Ding Y, et al. Screening for Coding Variants in FTO and SH2B1 Genes in Chinese Patients with Obesity. PloS one. 2013; 8
53. Deliard S, Panossian S, Mentch FD, Kim CE, Hou C, Frackelton EC, et al. The missense variation landscape of FTO, MC4R, and TMEM18 in obese children of African Ancestry. Obesity. 2013; 21:159–163. [PubMed: 23505181]
54. Zheng Z, Hong L, Huang X, Yang P, Li J, Ding Y, et al. Screening for coding variants in FTO and SH2B1 genes in Chinese patients with obesity. PloS one. 2013; 8:e67039. [PubMed: 23825611]
55. Hubacek JA, Stanek V, Gebauerova M, Pilipcincova A, Dlouha D, Poledne R, et al. A FTO variant and risk of acute coronary syndrome. Clinica chimica acta; international journal of clinical chemistry. 2010; 411:1069–1072.
56. Pausova Z, Syme C, Abrahamowicz M, Xiao Y, Leonard GT, Perron M, et al. A Common Variant of the Fto Gene Is Associated Not Only with Increased Adiposity but Also Elevated Blood Pressure in French-Canadian Adolescents. J Hypertens. 2009; 27:S166–S166.
57. Wehr E, Schweighofer N, Moller R, Giuliani A, Pieber TR, Obermayer-Pietsch B. Association of FTO gene with hyperandrogenemia and metabolic parameters in women with polycystic ovary syndrome. Metabolism: clinical and experimental. 2010; 59:575–580. [PubMed: 19913856]
58. Cai X, Liu C, Mou S. Association between fat mass- and obesity-associated (FTO) gene polymorphism and polycystic ovary syndrome: a meta-analysis. PloS one. 2014; 9:e86972. [PubMed: 24466303]

Author Manuscript Author Manuscript Author Manuscript Author Manuscript

59. Elks CE, Perry JRB, Sulem P, Chasman DI, Franceschini N, He CY, et al. Thirty new loci for age at menarche identified by a meta-analysis of genome-wide association studies. Nat Genet. 2010; 42:1077–U1073. [PubMed: 21102462]
60. Benedict C, Jacobsson JA, Ronnemaa E, Sallman-Almen M, Brooks S, Schultes B, et al. The fat mass and obesity gene is linked to reduced verbal fluency in overweight and obese elderly men. Neurobiol Aging. 2011:32.
61. Keller L, Xu W, Wang HX, Winblad B, Fratiglioni L, Graff C. The obesity related gene, FTO, interacts with APOE, and is associated with Alzheimer's disease risk: a prospective cohort study. Journal of Alzheimer's disease : JAD. 2011; 23:461–469. [PubMed: 21098976]
62. Alosco ML, Benitez A, Gunstad J, Spitznagel MB, McCaffery JM, McGeary JE, et al. Reduced memory in fat mass and obesity-associated allele carriers among older adults with cardiovascular disease. Psychogeriatrics : the official journal of the Japanese Psychogeriatric Society. 2013; 13:35–40. [PubMed: 23551410]
63. Melka MG, Gillis J, Bernard M, Abrahamowicz M, Chakravarty MM, Leonard GT, et al. FTO, obesity and the adolescent brain. Human molecular genetics. 2013; 22:1050–1058. [PubMed: 23201753]
64. Stratakis CA, Lafferty A, Taymans SE, Gafni RI, Meck JM, Blancato J. Anisomastia associated with interstitial duplication of chromosome 16, mental retardation, obesity, dysmorphic facies, and digital anomalies: Molecular mapping of a new syndrome by fluorescent in situ hybridization and microsatellites to 16q13 (D16S419-D16S503). J Clin Endocr Metab. 2000; 85:3396–3401. [PubMed: 10999840]
65. van den Berg L, Delemarre-van de Waa H, Han JC, Ylstra B, Eijk P, Nesterova M, et al. Investigation of a Patient With a Partial Trisomy 16q Including the Fat Mass and Obesity Associated Gene (FTO): Fine Mapping and FTO Gene Expression Study. Am J Med Genet A. 2010; 152A:630–637. [PubMed: 20186806]
66. Osborn DP, Roccasecca RM, McMurray F, Hernandez-Hernandez V, Mukherjee S, Barroso I, et al. Loss of FTO antagonises Wnt signaling and leads to developmental defects associated with ciliopathies. PloS one. 2014; 9:e87662. [PubMed: 24503721]
67. De Calisto J, Araya C, Marchant L, Riaz CF, Mayor R. Essential role of non-canonical Wnt signalling in neural crest migration. Development. 2005; 132:2587–2597. [PubMed: 15857909]
68. Pattnaik NM, Montes A, Hughes LB, Zilversmit DB. Cholesteryl ester exchange protein in human plasma isolation and characterization. Biochimica et biophysica acta. 1978; 530:428–438. [PubMed: 212110]
69. Lamarche B, Uffelman KD, Carpentier A, Cohn JS, Steiner G, Barrett PH, et al. Triglyceride enrichment of HDL enhances in vivo metabolic clearance of HDL apo A-I in healthy men. The Journal of clinical investigation. 1999; 103:1191–1199. [PubMed: 10207171]
70. Inazu A, Brown ML, Hesler CB, Agellon LB, Koizumi J, Takata K, et al. Increased high-density lipoprotein levels caused by a common cholesteryl-ester transfer protein gene mutation. The New England journal of medicine. 1990; 323:1234–1238. [PubMed: 2215607]
71. Brown ML, Inazu A, Hesler CB, Agellon LB, Mann C, Whitlock ME, et al. Molecular basis of lipid transfer protein deficiency in a family with increased high-density lipoproteins. Nature. 1989; 342:448–451. [PubMed: 2586614]
72. Maruyama T, Sakai N, Ishigami M, Hirano K, Arai T, Okada S, et al. Prevalence and phenotypic spectrum of cholesteryl ester transfer protein gene mutations in Japanese hyperalphalipoproteinemia. Atherosclerosis. 2003; 166:177–185. [PubMed: 12482565]
73. Nagano M, Yamashita S, Hirano K, Takano M, Maruyama T, Ishihara M, et al. Molecular mechanisms of cholesteryl ester transfer protein deficiency in Japanese. Journal of atherosclerosis and thrombosis. 2004; 11:110–121. [PubMed: 15256762]
74. Koizumi J, Mabuchi H, Yoshimura A, Michishita I, Takeda M, Itoh H, et al. Deficiency of serum cholesteryl-ester transfer activity in patients with familial hyperalphalipoproteinaemia. Atherosclerosis. 1985; 58:175–186. [PubMed: 3937535]
75. Funke H, Wiebusch H, Fuer L, Muntoni S, Schulte H, Assmann G. Identification of Mutations in the Cholesterol Ester Transfer Protein in Europeans with Elevated High-Density-Lipoprotein Cholesterol. Circulation. 1994; 90:241–241. [PubMed: 8026004]

Author Manuscript Author Manuscript Author Manuscript Author Manuscript

76. Teh EM, Dolphin PJ, Breckenridge WC, Tan MH. Human plasma CETP deficiency: identification of a novel mutation in exon 9 of the CETP gene in a Caucasian subject from North America. Journal of lipid research. 1998; 39:442–456. [PubMed: 9508004]
77. Rhyne J, Ryan MJ, White C, Chimonas T, Miller M. The two novel CETP mutations Gln87X and Gln165X in a compound heterozygous state are associated with marked hyperalphalipoproteinemia and absence of significant coronary artery disease. J Mol Med-Jmm. 2006; 84:647–650.
78. van der Steeg WA, Hovingh GK, Klerkx AHEM, Hutten BA, Nootenboom IC, Levels JHM, et al. Cholesteryl ester transfer protein and hyperalphalipoproteinemia in Caucasians. Journal of lipid research. 2007; 48:674–682. [PubMed: 17192423]
79. Calabresi L, Nilsson P, Pinotti E, Gomaraschi M, Favari E, Adorni MP, et al. A novel homozygous mutation in CETP gene as a cause of CETP deficiency in a caucasian kindred. Atherosclerosis. 2009; 205:506–511. [PubMed: 19200546]
80. de Grooth GJ, Klerkx AHEM, Stroes ESG, Stalenhoef AFH, Kastelein JJP, Kuivenhoven JA. A review of CETP and its relation to atherosclerosis. Journal of lipid research. 2004; 45:1967–1974. [PubMed: 15342674]
81. Choi M, Scholl UI, Ji W, Liu T, Tikhonova IR, Zumbo P, et al. Genetic diagnosis by whole exome capture and massively parallel DNA sequencing. Proceedings of the National Academy of Sciences of the United States of America. 2009; 106:19096–19101. [PubMed: 19861545]
82. Clark VE, Erson-Omay EZ, Serin A, Yin J, Cotney J, Ozduman K, et al. Genomic analysis of non-NF2 meningiomas reveals mutations in TRAF7, KLF4, AKT1, and SMO. Science. 2013; 339:1077–1080. [PubMed: 23348505]
83. Sathirapongsasuti JF, Lee H, Horst BA, Brunner G, Cochran AJ, Binder S, et al. Exome sequencing-based copy-number variation and loss of heterozygosity detection: ExomeCNV. Bioinformatics. 2011; 27:2648–2654. [PubMed: 21828086]
84. Dennis G Jr, Sherman BT, Hosack DA, Yang J, Gao W, Lane HC, et al. DAVID: Database for Annotation, Visualization, and Integrated Discovery. Genome biology. 2003; 4:P3. [PubMed: 12734009]
85. Zuber TJ. Punch biopsy of the skin. Am Fam Physician. 2002; 65:1155. [PubMed: 11925094]
86. Levitt J, Bernardo S, Whang T. How to Perform a Punch Biopsy of the Skin. New Engl J Med. 2013; 369:E13–E13. [PubMed: 24024863]
87. Church C, Lee S, Bagg EA, McTaggart JS, Deacon R, Gerken T, et al. A mouse model for the metabolic effects of the human fat mass and obesity associated FTO gene. Plos Genet. 2009; 5:e1000599. [PubMed: 19680540]
88. Schmittgen TD, Livak KJ. Analyzing real-time PCR data by the comparative C(T) method. Nat Protoc. 2008; 3:1101–1108. [PubMed: 18546601]

Author Manuscript Author Manuscript Author Manuscript Author Manuscript

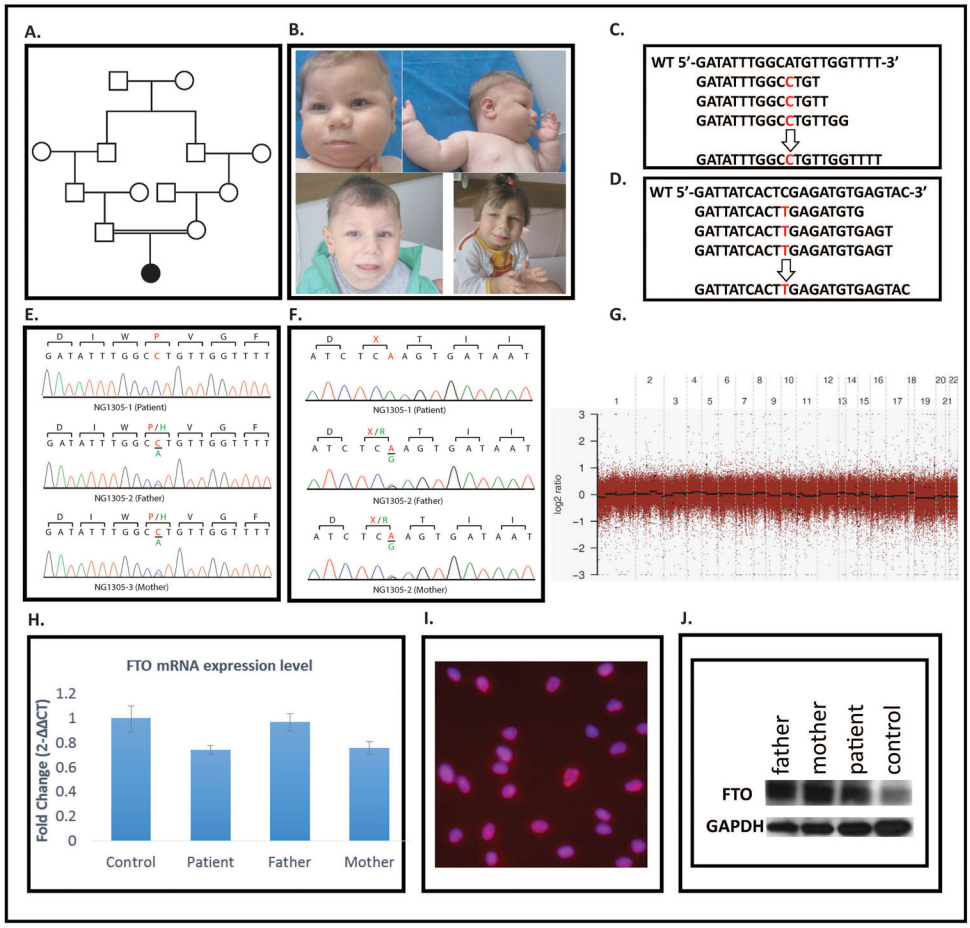

Figure 1. I Phenotypic and molecular studies has been performed on materials obtained from index patient, parents and control samples

A. Pedigree of the family. **B.** Clinical pictures of the patient (upper right panels) when she was 9 month-old (upper panels), 2 and half years old (left lower panel) and 4 and nine month-old (right lower panel). **C and D.** Representative sequence alignment figures cover the mutations in *FTO* and *CETP*, respectively. The top line in each panel represents the non-mutated reference sequence. The subsequent lines below the reference lines depict the results from exome sequence. Each line represents a distinct coverage read. Mean 20x coverage of all bases was above 81% for index patient. **E and F.** Chromatogram illustrations of *FTO* and *CETP* obtained via Sanger sequencing analysis of the index patient analyzed via whole-exome sequencing (NG1305-1) and her parents. Note that the respective mutations identified via whole-exome sequencing were confirmed as homozygous mutations in the index patient and as heterozygous in her parents. DNA from healthy individuals was also Sanger sequenced and these results are included as controls. **G. CNV Segment Detection of NG1305-1:** The log ratio comparing NG1305-1 and control sequence depths of coverage for each exon are depicted as gray dots. The black lines demonstrate regions of segmented copy neutral events, green lines are segmented deletion events and red lines are amplification events. **H.** mRNA levels of *FTO* in fibroblast cells were extracted from homozygous patient, heterozygous parents and control individual-same ethnicity and without a sequence variant-

Author Manuscript Author Manuscript Author Manuscript Author Manuscript

were analyzed using RT-PCR. **I**. The figure depicts FTO staining in patient fibroblasts. Significant nuclear accumulation is noted. **J.** Western blot of FTO and as an internal control GAPDH in patient, parental and control cells. No difference was detected.

Author Manuscript Author Manuscript Author Manuscript Author Manuscript

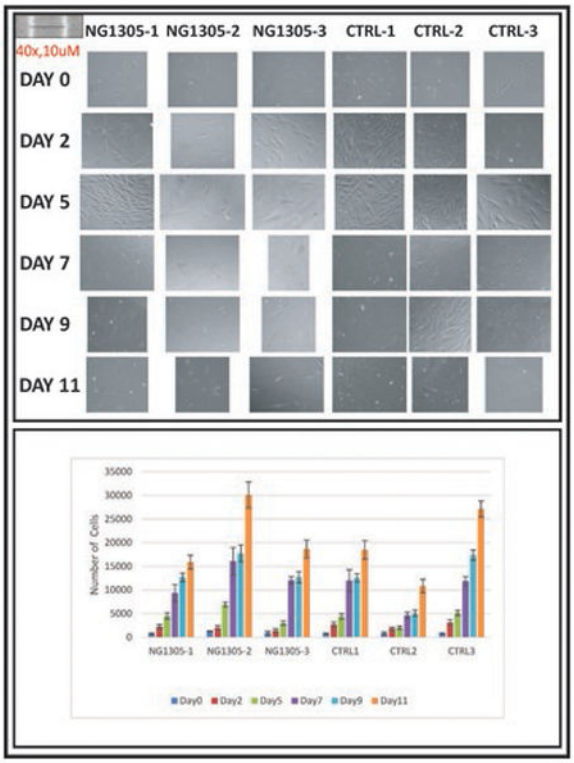

Figure 2. I Phenotypic and proliferation comparisons of fibroblasts extracted from index case, parents and control subjects

Upper panel shows comparison of fibroblast morphology of the patient, her parents and control fibroblasts. Images were taken after 2nd, 5th, 7th, 9th and 11thdays incubation under 20x objectives**. Lower panel** compares number of cells versus time in each study subject and there is no statistically difference between the patient and control samples.

Author Manuscript Author Manuscript Author Manuscript Author Manuscript

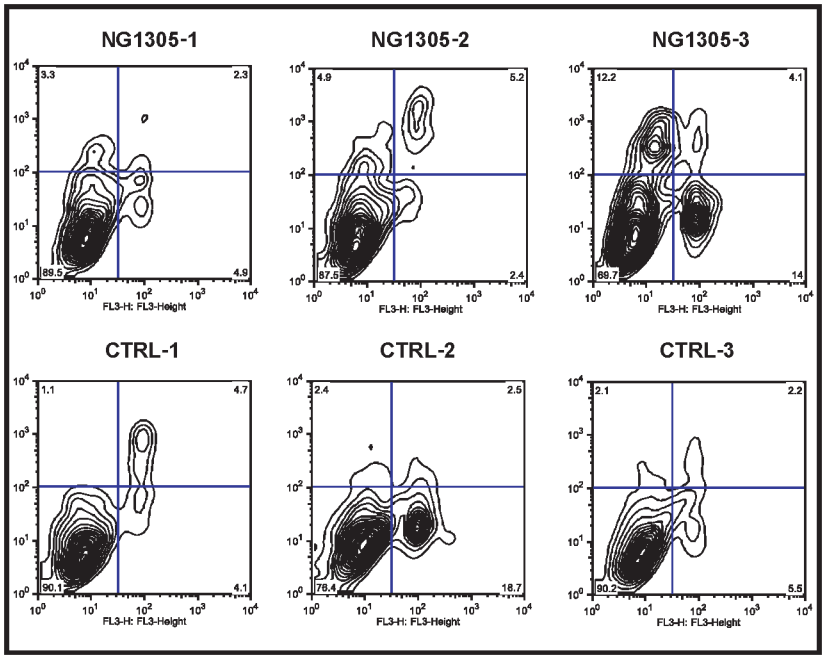

Figure 3. I The flow cytometric analysis of apoptosis in fibroblast cells after three days incubation using FITC-annexin V and 7AAD double staining

Quadrant analysis of the gated cells in FL-1 versus FL-3 channels was from 1,000 events. Annexin V+/7AAD− (lower left quadrant) areas stand for early apoptotic cells, and Annexin V+/7AAD+ (upper right quadrant) areas stand for late apoptotic or necrotic cells.